Media Engineering and Technology Faculty
German University in Cairo

Embedded System for Ultrasound Breast Cancer Diagnosis

Bachelor Thesis

Author:	Ahmed Mahmoud Kamal
Supervisors:	Dr. Shereen Moataz Afifi,
	Prof. Dr. Mohammed Abdel-Megeed Salem,
	Eng. Radwa Essam Taha
Submission Date:	19 May, 2024

Media Engineering and Technology Faculty
German University in Cairo

Embedded System for Ultrasound Breast Cancer Diagnosis

Bachelor Thesis

Author:	Ahmed Mahmoud Kamal
Supervisors:	Dr. Shereen Moataz Afifi,
	Prof. Dr. Mohammed Abdel-Megeed Salem,
	Eng. Radwa Essam Taha
Submission Date:	19 May, 2024

This is to certify that:

(i) the thesis comprises only my original work toward the Bachelor Degree

(ii) due acknowledgment has been made in the text to all other material used

Ahmed Mahmoud Kamal
19 May, 2024

Acknowledgments

I would like to express my sincere gratitude to my advisors, Dr. Shereen Afifi, Prof. Dr. Mohammed Salem, and Eng. Radwa Taha, for their invaluable guidance and assistance throughout this research. Special thanks to my colleagues and friends for their continuous support. Finally, I am deeply grateful to my family for their unwavering love and support.

Abstract

Early diagnosis of breast cancer plays a crucial role in improving patient outcomes and survival rates. The integration of artificial intelligence (AI) in medical imaging opens up new opportunities for enhancing diagnostic accuracy and accessibility. Consequently, an accurate, affordable, and portable breast diagnosis system would improve the survival rates and overall quality of life for many patients. While many studies have reported high accuracy using convolutional neural networks (CNNs) on limited datasets, the ability of these models to generalize effectively remains a concern. In this study, five diverse datasets (BUSI, BUS_UC, BUS_WHU, BUS-UCLM, and BUSBRA) were utilized for training, and an extra dataset called Dataset B was reserved for system evaluation. The proposed system adopts a two-stage classification approach, distinguishing between abnormal and normal images initially, followed by benign and malignant classification if abnormalities are detected. The system features two highly advanced pretrained models: ResNet101 and InceptionV3. The system has achieved accuracies of 99.31% and 86% for stage 1 and stage 2 models, respectively, and 88% when evaluating the whole system. To enhance accessibility, the models were converted to TFLite and deployed on a Raspberry Pi 3 with a user-friendly graphical interface for instant diagnosis.

This research was accepted for funding by the ITIDA ITAC program.

Contents

List of Figures

List of Tables

Chapter 1

Introduction

1.1 Motivation

In 2020, the World Cancer Research Fund reported that breast cancer is the most common type of cancer in the world, with over 2 million cases, breast cancer alone makes up 12.5% of all new cases recorded in 2020 and 25.8% of new cases in women [37]. The decision to pursue this project was motivated by the need for affordable, improved, and accessible methods of diagnosing breast cancer, which can be used by individuals inside and outside the medical profession. With that being said, early detection of breast cancer significantly improves the chance of survival, however around 50% of cancers are still only detected at a later stage [38]. There is a clear incentive to develop innovative solutions that can reach a wider population. By focusing on affordability, accuracy and portability, this project aims to help more people get access to diagnostic services for breast cancer, which will make healthcare better for everyone.

Furthermore, recent advances in artificial intelligence and machine learning offer a great opportunity to change how we diagnose breast cancer. With these technologies, we can create tools that are not only affordable but also accurate at spotting cancer early. By using AI to analyze ultrasounds, we can improve the chances of finding early signs of cancer that might be hard for humans to see. This project seeks to use these innovations to develop a comprehensive diagnostic system that can be deployed in various settings, from urban hospitals to patients. By making cutting-edge technology accessible to a wider audience, we can contribute to the early detection and treatment of breast cancer, ultimately saving lives and reducing healthcare disparities.

1.2 Problem Statement

This study aims to develop a deep learning model for the classification and diagnosis of breast cancer using ultrasound images by leveraging the newest deep learning models available. Specifically, we will use existing models that are already trained and adjust them for breast cancer diagnosis, applying Transfer Learning concepts to adapt their capabilities to our specific task. we aim to make the classification process better and more accurate. The primary objective is to find whether an ultrasound shows a tumor or not, if it does it should analyze the tumor and output if its cancerous or not. The model will be trained using various datasets to increase it's ability to generalize to ultrasound images taken with different devices. The finalized model will be deployed onto a Raspberry Pi device. This implementation will make it easy to connect with handheld ultrasound devices, allowing for immediate diagnosis of breast cancer. Additionally, the model's output will be displayed on a screen, providing accessible results to end-users.

1.3 Objectives

The objectives of this work are:

- Design and train a deep learning model architecture tailored for breast cancer classification using ultrasound images.
- Integrate the model with a Raspberry Pi for real-time diagnosis of breast cancer.
- Develop a user-friendly interface to display model predictions and diagnostic results for healthcare professionals and end-users.
- Overall build an efficient device for early diagnosis of breast cancer.

1.4 Thesis Outline

In this thesis, we will be discussing the development and implementation of a deep learning model for the classification and diagnosis of breast cancer utilizing ultrasound images. In Chapter 1 we discuss the importance of innovative solutions for early diagnosis of breast cancer and the aim of this research. In Chapter 2 we discuss the definitions and applications of Deep Learning and Transfer Learning and how these techniques can be effectively used to enhance the performance of the developed model even with small datasets, we also discuss classification which is a very important computer vision concept, and finally we discuss previous studies including the models and datasets used and their results. In Chapter 3, we provide a detailed overview of the methodology employed in this study. This includes data preprocessing techniques, model architecture, training procedure, and evaluation metrics. In Chapter 4 we will discuss the results of our proposed model. This chapter will present a thorough analysis of the model's performance, including metrics such as accuracy, precision, recall, and F1-score. In the final chapter, Chapter 5, we provide a conclusion of the work done by this paper and how it can be improved upon in the future.

- **Concept Overview:** A brief explanation of all technologies used throughout the paper.
- **Literature Review:** A summary of some of the work done previously and a comparison between them to find the best approach in this study.
- **Methodology:** Workflow overview on how the project was implemented and how the environment developed could be replicated.
- **Results:** This section contains the results of the proposed model's performance and accuracy.
- **Conclusion:** A brief discussion of what was achieved in this paper, and the future work that could be done to excel the results and further development.

Chapter 2

Background

2.1 Concepts overview

2.1.1 Ultrasound

Ultrasound, or ultrasonography, is a medical imaging technique that uses high-frequency sound waves to create images of the inside of the body. It is commonly used to monitor fetal development, assess heart function, and diagnose conditions in organs like the liver, kidneys, and in detecting breast cancer. It is generally considered a safer option than other imaging methods such as Mammography because it does not use ionizing radiation which may lead to damaging tissue and DNA in genes after long exposures.

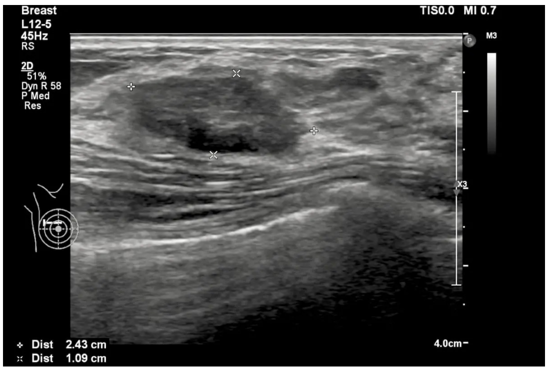

Breast Ultrasound [42]

Obstetric Ultrasound [43]

Figure 2.1: Examples of Ultrasound images.

2.1.2 Deep Learning

Deep learning, a subset of machine learning, enables computers to learn from huge datasets, discovering intricate patterns and making intelligent decisions without explicit programming. Artificial Neural Networks learn from labeled datasets, adjusting internal parameters iteratively using optimization techniques such as gradient descent, aiming to minimize the difference between predicted and actual outputs. Through this iterative process, deep learning models can capture complex relationships within the data that can be impossible for a human to capture, allowing them to generalize and make accurate predictions on unseen examples.

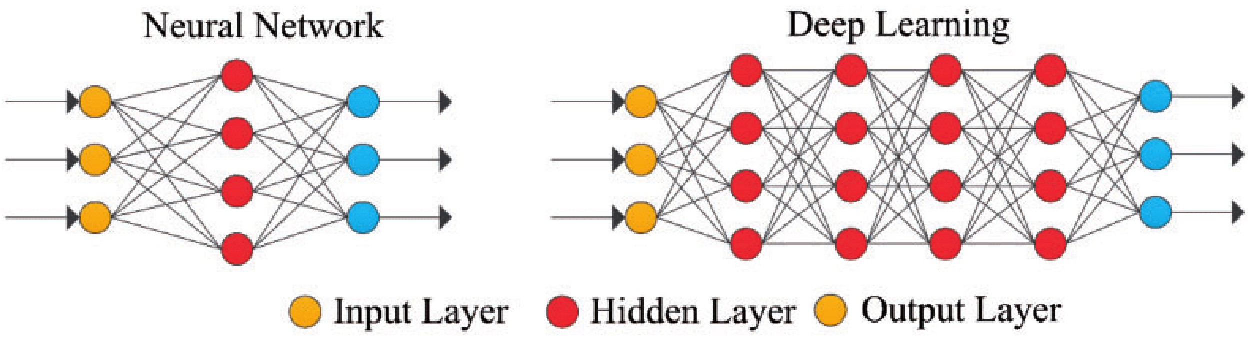

Figure 2.2: Neural Networks & Deep Learning [40]

2.1.3 Transfer Learning

Transfer learning, on the other hand, uses knowledge gained from solving one problem and applies it to a different but related task. Instead of starting the learning process from scratch, it initializes the model with pre-trained weights obtained from a previously trained model, fine-tuning it to adapt to the new task. This approach reduces the amount of data needed to train the model, which is very helpful in scenarios where data is scarce.

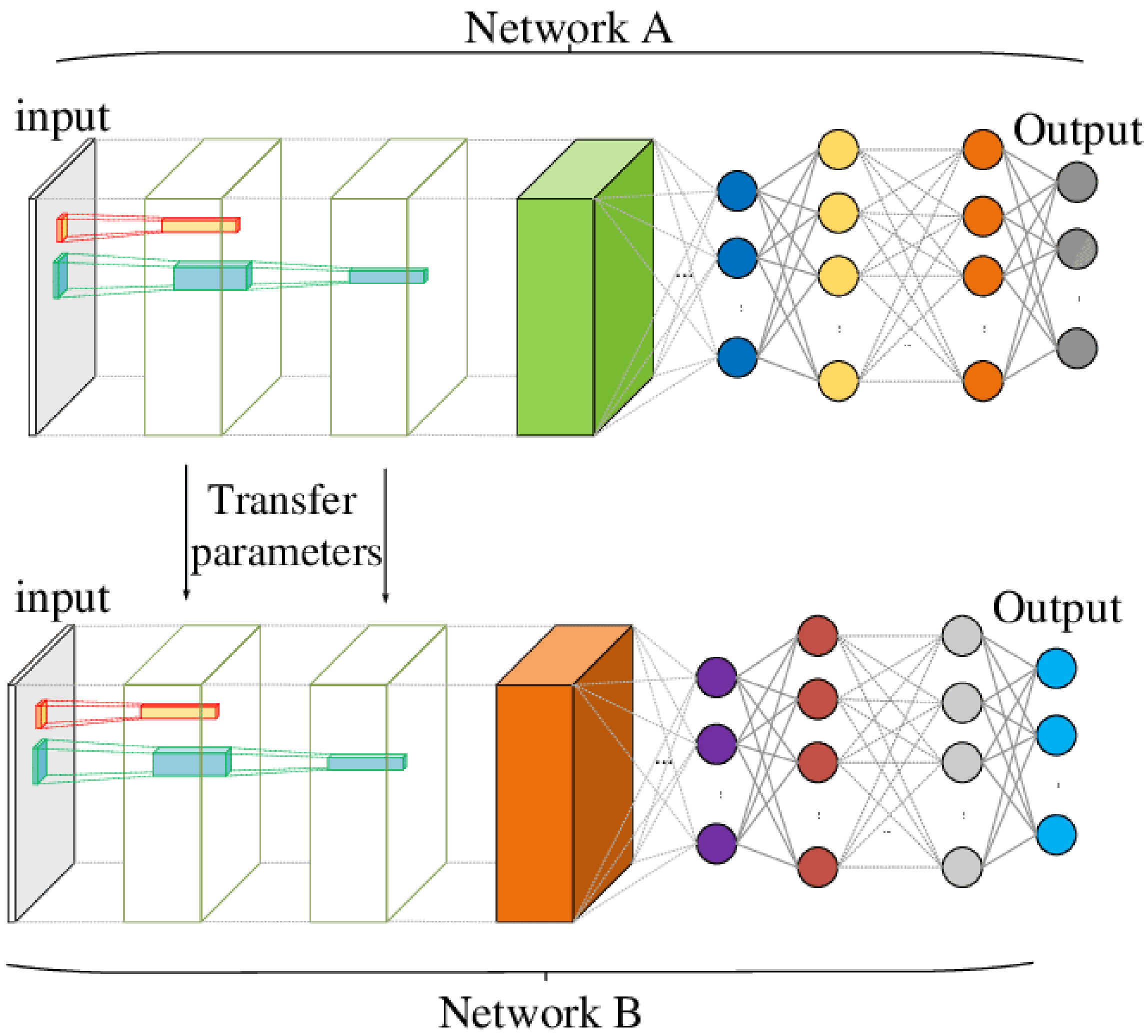

Figure 2.3: Illustration of Transfer Learning in Deep Learning [41]

2.1.4 Classification

Classification is a foundational task in machine learning that involves assigning predefined labels or categories to input data based on its features. The process involves training a model using labeled data, where each data point is associated with a known class. The trained model learns patterns in the data to make predictions on unseen data, accurately classifying them into the appropriate categories. Through classification, machines can automate decision-making processes, enabling applications in many fields such as healthcare.

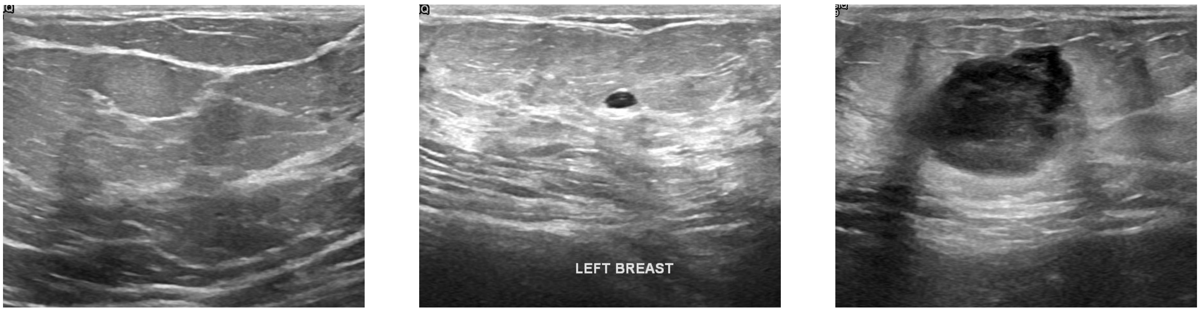

Normal Benign Malignant

Figure 2.4: Samples of all three classes in the BUSI dataset. [31]

2.1.5 Loss Function

A loss function measures how well a machine learning model is performing by comparing its predictions to the actual target values. It calculates the difference between predicted and actual values, providing a measure of the model's performance during training. Common loss functions include Dice Loss for segmentation problems and categorical or binary cross-entropy for classification problems.

2.1.6 Optimizer

An optimizer is an algorithm used to minimize the loss function during the training of a machine learning model. It adjusts the model's parameters (weights and biases) iteratively based on the gradients of the loss function with respect to those parameters. Popular optimizers include stochastic gradient descent (SGD), Adaptive Moment Estimation (Adam), and RMSprop.

2.1.7 Activation Functions

ReLU (Rectified Linear Unit)

ReLU is an activation function used in neural networks, it introduces non-linearity by outputting zero for negative input values and the input value itself for positive input values. Mathematically, ReLU is defined as $f(x) = \max(0, x)$.

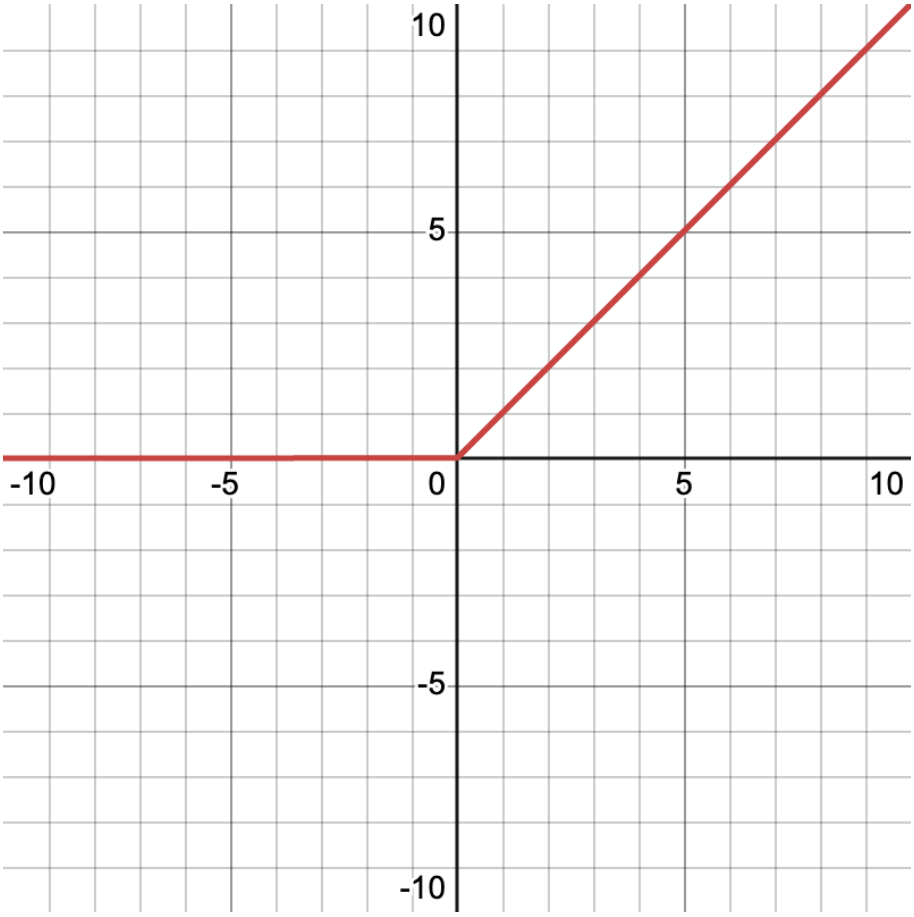

Figure 2.5: Graph of the ReLU Function.

Sigmoid Function

The sigmoid function is a non-linear activation function commonly used in binary classification problems. It maps input values to the range [0, 1], making it suitable for predicting probabilities. Mathematically, the sigmoid function is defined as $f(x) = \frac{1}{1+e^{-x}}$.

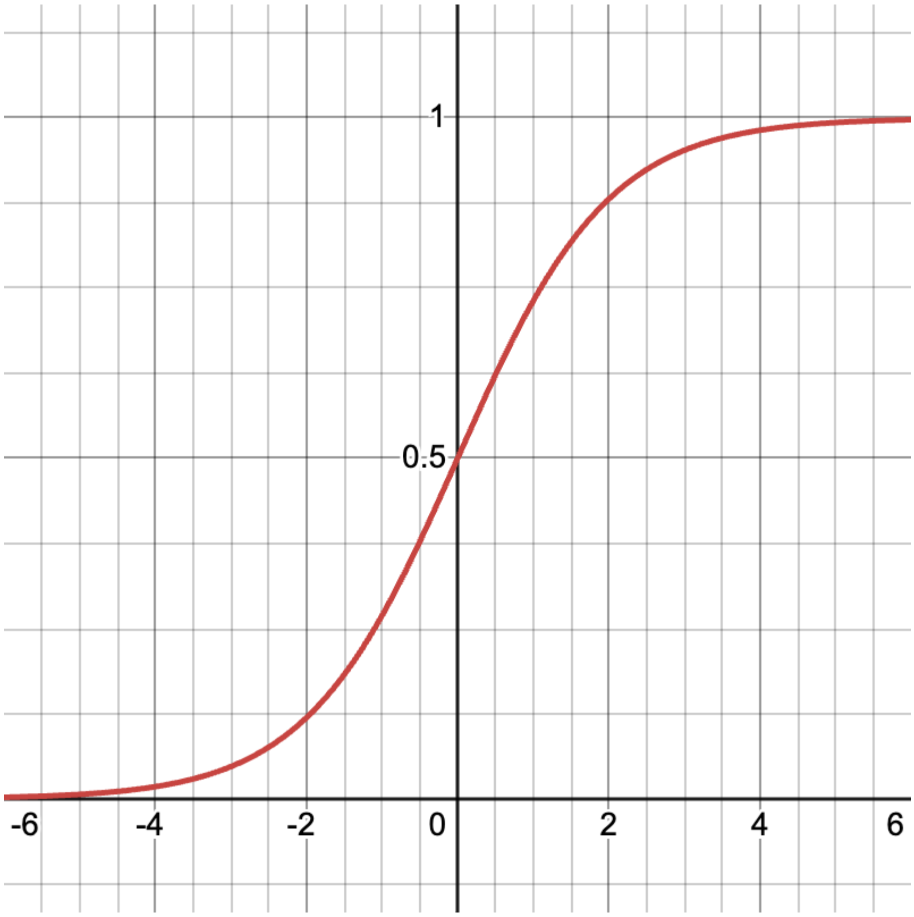

Figure 2.6: Graph of the Sigmoid Function.

Both the sigmoid and ReLU graphs were generated using Desmos graphing calculator [47]. Desmos provides a user-friendly interface for creating mathematical visualizations.

2.1.8 Overfitting

Overfitting occurs when a machine learning model learns the training data too well, capturing noise and random fluctuations rather than the underlying pattern. As a result, the model performs well on the training data but poorly on unseen data, showing poor generalization.

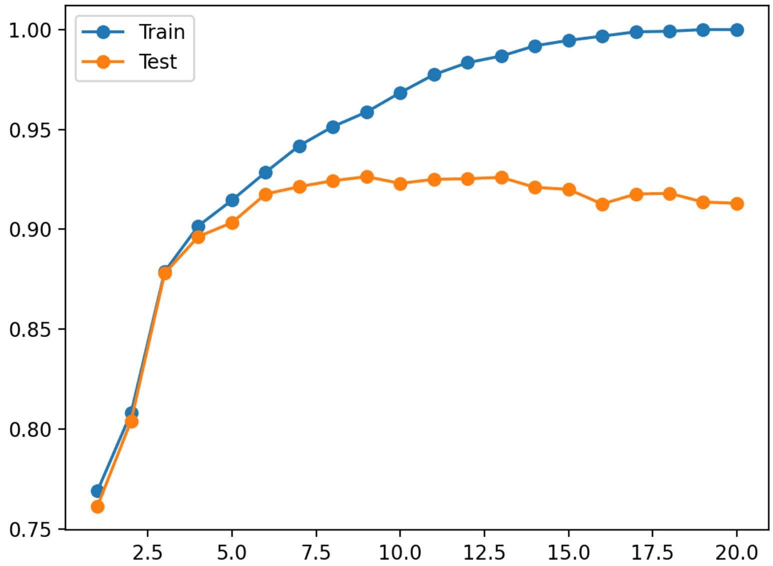

Figure 2.7: Example of the Accuracy results of a high variance model. [45]

2.1.9 Regularization

Regularization techniques are used to prevent overfitting by adding penalties to the model's parameters. L2 regularization, also known as weight decay, adds a penalty to the loss function based on the squared values of the model's weights. This encourages smaller weight values and helps prevent overfitting by reducing model complexity.

2.1.10 Batch Normalization

Batch normalization is a technique used to improve the training stability and performance of neural networks. It normalizes the activations of each layer by adjusting and scaling them to have zero mean and unit variance. This helps prevent issues such as vanishing gradients.

2.2 Literature Review

2.2.1 Discussion

Models used for Classification: Inception

Nasim Sirjani et al. (2023) [4] proposed a new improved InceptionV3 architecture, they converted the InceptionV3 modules to residual inception ones, increased their number, and altered the hyperparameters, they used five datasets including two prepared from different imaging centers. They reported 81% accuracy.

Tomoyuki Fujioka et al. (2019) [7] used GoogLeNet which is essentially InceptionV1, the dataset consisted of multi-view images of benign and malignant tumors that sums up to 947 images. The accuracy achieved by this approach is 92.5%.

Yi Wang et al. (2020) [13] proposed an improved InceptionV3 CNN which retains the convolutional structure as the backbone for lesion feature extraction and The fully-connected layers are redesigned, and a global average pooling layer is added to the output feature maps for efficient feature extraction. They used a custom dataset of 316 Images and reported an AUC of 94.68%.

Shao-Hua Chen et al. (2023) [21] used GoogLeNet on a 880 Images dataset and reported an accuracy of 93.23%. They compared the model to AlexNet which achieved an accuracy of 87.02%.

Xiaofeng Qi et al. (2021) [25] proposed a new system for mobile phones that uses stacked denoising autoencoders, GAN, and DCNN to reduce noise, classify images, and detect anomalies. The system was trained on 18,225 ultrasonography images and 2,416 ultrasound reports and achieved an accuracy of 87%.

Models used for Classification: ResNet

Hiroki Tanaka et al. (2019) [3] introduced an ensemble method by combining VGG19 and ResNet152, they used a dataset consisting of 1536 images collected from 17 facilities in Japan. The paper reported a View Level accuracy of 86% and a Mass Level accuracy of 89%.

In the paper published by Se Woon Cho et al. (2022) [10], they proposed a multi-stage approach for segmentation, the first stage is classification using an ensemble of DenseNet121 and ResNet101, the proposed ensemble model is called BTEC-Net and the classification was used to predict abnormal ultrasound images to later be used in stage 2 which is segmentation using UNet. They used the dataset BUSI and reported 99.487% accuracy in Stage 1.

Ikram Ben Ahmed et al. (2022) [14] published a study that uses ResNet50 using pretrained weights, they used 780 Images from the BUSI Dataset and achieved 93.65% Accuracy.

Xuejun Qian et al. (2021) [19] proposed a multipathway deep convolutional neural network using ResNet-18 with a SENet module for breast cancer risk prediction from multimodal ultrasound images. The model was trained on 10,815 images, achieving an AUC of 0.923.

Models used for Classification: NASNet

Walid Al-Dhabyani et al. (2019) [6] compared five deep learning models AlexNet, VGG16, Inception, ResNet, NASNet, using pretrained weights for the latter four. They also tested on four forms of data samples, the best results were achieved by using a pretrained NASNet Model on a combination of BUSI and Dataset B with DAGAN Augmentation, which was 99% Accuracy.

Models used for Segmentation and Object Detection

Stage 2 of the paper published by Se Woon Cho et al. (2022) [10] involved using UNet for segmenting abnormal images, as mentioned in the ResNets section 2.2.1, they used BUSI, they achieved an IoU of 77.094% and 97.253% pixel accuracy.

Aleksandar Vakanski et al. (2020) [17] compared Attention Enriched U-Net-SA and Attention Enriched U-Net-SA-C, they used a custom dataset collected from three hospitals in China and achieved an accuracy of 97.9% and a Dice Similarity Coefficient of 0.901.

Yujie Li et al. (2022) [20] implemented a Deep Learning model called BUSnet for Breast cancer detection in ultrasound images, they used the BUSI dataset and reported an accuracy of 65.1%.

Shahed Hossain et al. (2023) [23] used a Hybrid Attention UNet, CNN: RKO-UNet-13, with the BUSI dataset and achieved an accuracy of 98.41%.

Sushma B. & Aparna Pulikala (2024) [24] used a CNN with Attention Aggregation Feature Clustering Module (AAPFC) BUSnet for detection of tumors in ultrasounds. They used the BUSI dataset and reported an accuracy of 96%.

Models Deployed on an Edge Device

Shahirah Zahir et al. (2021) [26] used VGG16 for Histopathological Images classification, the dataset used consisted of 7909 Histopathological Images and the device used was a Raspberry Pi 3 B+, the GUI was created using AppJar and they reached an accuracy of 79.12%.

Mahmut Taha Yazici et al. (2018) [27] compared two models , SVM and RF, on multiple datasets for classification, using a Raspberry Pi 3 B, achieving an accuracy of 84.09% using SVM and 92.34% using RF.

Bharath Sudharsan et al. (2021) [28] proposed a framework for breast cancer diagnosis using the Wisconsin Dataset, which is 567 Rows, they didn't mention the device used but the accuracy achieved was 83%.

Brian H. Curtin & Suzanne J. Matthews (2019) [29] used a simple CNN to train on 3600 Images divided across 3 classes, they used a Raspberry Pi 3 B+ and achieved 72-77% Accuracy.

Lana Alhaj Hussain et al. (2020) [30] deployed an InceptionV3 model trained on 33984 images on a Raspberry Pi 4 B, achieving 94% Accuracy and only two seconds per image.

Additional Studies Reviewed

Ishak Pacal (2022) [1] used a Vision Transformer (ViT) with 780 images from BUSI and increased their number using data augmentation techniques, achieving 88.6% accuracy and 90.1% precision. In the same year, Kiran Jabeen et al. [8] proposed a system that uses a CSVM classified with Binary Gray Wolf and Differential Evolution Opimizations, they also used BUSI with data augmentation and they reported an accuracy of 99.18%, Precision, Sensitivity and F1-Score of 99.06%.

Jianming Li et al. (2021) [2] collected 7969 Images from 1970 patients with 2071 nodules, 1271 of them were malignant, they used RetinaNet and achieved 91% accuracy.

Anton S Becker et al. (2018) [5] used an industrial grade image analysis software called ViDi Suite v.2.0, they used a custom dataset including 637 ultrasound Images and reported an AUC of 84%.

Kenichi Inoue et al. (2017) [9] impleneted a CNN with 10 hidden layers they trained and tested it using a custom dataset collected in Japan consisting of 818 Images and after using data augmentation they reached 2604 Images. The accuracy reported was 95.4%.

Madhusudan G. Lanjewar et al (2024) [11] proposed using three TL models, MobileNetV2, ResNet50 and VGG16, were combined with LSTM to extract the features from Ultrasound Images, they used the Kaggle Breast USIs containing 1578 Images and achieved an F1-Score of 99.0%.

In the study published by Ronghui Tian et al. (2024) [12] They employed conventional radiomics and transfer learning, using models like ResNet50 and MNASNet, to classify breast tumor ultrasound images. They collected 1050 Images in China for training and for testing they used BUSI Dataset in addition to 105 Images from Liaoning Cancer Hospital in China. They achieved 94% accuracy.

Yaozhong Luo et al. (2023) [15] introduced a new strategy for breast ultrasound classification, generating multi-resolution tumor-centered images (TCIs) for multi-view learning. They used 1702 Images and reported a 92.12% accuracy.

Moi Hoon Yap et al. (2017) [16] published a study about using FCN-AlexNet on Dataseb B, they reported a True Positive Fraction of 0.93.

Mahmoud Ragab et al. (2022) [18] proposed an ensemble of VGG16, VGG19 and SqueezeNet + MLP, they used the BUSI dataset and reported 97.2% accuracy.

Yi-Cheng Zhu et al. (2020) [22] proposed a generic deep convolutional neural network (DCNN) architecture, TNet and BNet, trained with transfer learning for classifying thyroid and breast lesions in ultrasound images. They used a custom dataset containing 672 images and reported 86.5% accuracy for TNet and 89% accuracy for BNet.

Limitations

Many studies in this literature review relied on a limited number of datasets, often one or two, which may restrict their models' ability to generalize, leading to potential overfitting to specific dataset features and poor performance on unseen data. Additionally, a significant proportion of these studies used private datasets, which may prevent other researchers from replicating and building onto their results which could slow down further advancements in the field. In contrast, this project uses six different publicly available datasets collected from different countries, details on their preprocessing and usage can be found in chapters 4 and 5, also the model is tested on a completely unseen dataset to accurately measure its performance. Furthermore, despite the rising interest in deep learning in the medical field, there's a noticeable absence of studies specifically addressing breast cancer diagnosis on edge devices. This gap in research provides an opportunity for future investigations to examine the effectiveness and usefulness of deploying breast cancer diagnosis models on edge devices.

2.2.2 Literature Review Comparisons

Comparison of Deep Learning Models for Classification

Table 2.1: Summary of existing techniques for breast cancer classification.

Ref	Year	Models	Dataset	Results
[1]	2022	Vision Transformer (ViT)	BUSI 780 Images + Data Augmentation	ACC: 88.6% Precision: 90.1%
[2]	2021	CNN: RetinaNet	Custom Dataset 7969 Images	ACC: 91% — Sensitivity: 92% Specificity: 90%
[3]	2019	CNN: VGG19 + ResNet152	Custom Dataset 1536 Images 17 facilities in Japan	View Level: ACC: 86%, Sensitivity: 88.6%, Specificity: 83.1%, Precision: 85.4% Mass Level: ACC: 89%, Sensitivity: 90.9%, Specificity: 87%, Precision: 87.5%
[4]	2023	CNN: Improved InceptionV3	BUSI: 780 Images Dataset (B): 163 Images, UDIAT Diagnostic Center of the Parc Tauli Corporation, Spain Public Dataset 3: 86 Images, Thammasat University Hospital, Thailand Custom Dataset 1: 560 Images Custom Dataset 2: 150 Images, Dr. Gity Imaging Center	ACC: 81% — F1-Score: 80% Recall: 77% — Precision: 83% AUC: 81% — RMSE: 0.18
[5]	2018	SW: ViDi Suite v.2.0	Custom Dataset 637 Images	AUC: 84% — Specificity: 80.3% Sensitivity: 84.2%
[6]	2019	TL: NASNet	BUSI: 780 Images Dataset (B): 163 Images, UDIAT Diagnostic Center of the Parc Tauli Corporation, Spain	Using DAGAN & Traditional Augmentation: ACC: 99%
[7]	2019	CNN: GoogLeNet	Custom Dataset 947 Images	ACC: 92.5% — Specificity: 87.5% Sensitivity: 95.8% — AUC: 91.3%

[8]	2022	Classifier: CSVM Optimization: DE + BGWO	BUSI 780 Images	ACC: 99.18% — F1-Score: 99.06% Sensitivity: 99.06% — Precision: 99.06%
[9]	2017	CNN (10 Hidden Layers)	Custom Dataset 818 Images, Shonan Memorial Hospital, Japan 2604 Images After Data Augmentation	ACC: 95.4% — Specificity: 96.4% Sensitivity: 93.2%
[10]	2022	CNN: BTEC-Net DenseNet121 + ResNet101	BUSI 780 Images	ACC (Binary): 99.487% — Recall: 99.846% Precision: 99.538% — F1-Score: 99.692%
[11]	2024	TL + LSTM: MobileNetV2, ResNet50, and VGG16	Kaggle Breast USIs 1578 Images	AUC: 100% — K: 98.9% MCC: 98.9% — F1-Score: 99.0%
[12]	2024	TL: ResNet50, Inception-v3, DenseNet121, MNASNet, MobileNet	Dataset A: 1050 Images Collected in China Testing: BUSI: 780 Images + Dataset C: 105 Images, Liaoning Cancer Hospital in China	Balanced ACC: 94% — F1-Score: 94.2% Sensitivity: 89.9% — Specificity: 98.2% AUC: 98.1% — CI: 95%
[13]	2020	TL: Modified Inception-v3	Custom Dataset 316 Images JBNUH, South Korea	AUC: 94.68% Sensitivity: 88.6% — Specificity: 87.62%
[14]	2022	TL: ResNet-50	BUSI 780 Images	ACC: 93.65% — AUC: 90.5% Sensitivity: 83.33% — Specificity: 97.22%
[15]	2023	DCNN	Custom Dataset 1702 Images Cancer Center of Sun Yat-sen University	ACC: 92.12% Sensitivity: 95.31% — Specificity: 88.41% F1-score: 93.03% — AUC: 0.9743
[16]	2017	TL: FCN-AlexNet	Dataset (B): 163 Images	TPF: 0.93 — FPs/image: 0.18 F-measure: 0.88
[18]	2022	Ensemble: VGG-16, VGG-19, and SqueezeNet + MLP	BUSI Dataset 780 Images	Epoch-250 ACC: 97.2% — Precision: 95.39% Sensitivity: 96.01% — Specificity: 97.95 %
[19]	2021	Multipathway Deep Learning Model	Custom Dataset 10,815 Multimodal Multiview Images, 2 hospitals, China	AUC (Bimodal): 0.922 — AUC (Multimodal): 0.955
[21]	2023	TL: Modified GoogLeNet	Custom Dataset 880 Images Fujian Medical University in Quanzhou, China.	ACC: 93.23%
[22]	2020	TL, DCNN: TNet, BNet	Custom Dataset 672 Images Shanghai Pudong People's Hospital, China	ACC (TNet): 86.5% — ACC (BNet): 89% Sensitivity (TNet): 83.9% — Sensitivity (BNet): 88.2% Specificity (TNet): 88.6% — Specificity (BNet): 89.6%
[25]	2021	DeepCIs (Inception-v3) + DeepRec + DeepAti	Custom Dataset 18225 Images 3 Hospitals, China	ACC: 87% Sensitivity: 86% — Specificity: 88%

Comparison of Deep Learning Models for Segmentation and Detection

Table 2.2: Summary of existing techniques for breast cancer segmentation and detection.

Ref	Year	Models	Dataset	Results
[10]	2022	RFS-UNet	BUSI 780 Images	IoU: 77.094%
[17]	2020	Attention-Enriched: U-Net-SA vs U-Net-SA-C	Custom Dataset 510 Images, 3 hospitals, China	ACC: 97.9% — FPR: 9.2% ACC (C): 98% — FPR (C): 8.9%
[20]	2022	CNN: BUSnet	BUSI Dataset 780 Images	ACC: 65.1% — Precision: 65.1% Recall: 1 — F1-Score: 78.9%
[23]	2023	Hybrid Attention UNet (CNN: RKO-UNet-13)	BUSI Dataset 780 Images	ACC: 98.41%
[24]	2024	CNN with Attention Aggregation Feature Clustering Modile: AAPFC-BUSnet	BUSI Dataset 780 Images	ACC: 96% — Mean-IoU: 68% Specificity: 97% — Sensitivity: 82%

DL Models Deployed on Edge Devices Comparison

Table 2.3: Summary of existing deep learning models deployed on edge devices

Ref	Year	Models	Dataset	Hardware	Results
[26]	2021	TL: VGG16	BreakHis Database 7909 Images Histopathological Images	Raspberry Pi 3 B+, 1GB SRAM, ARM Cortex-A53 1.4GHz	ACC: 79.12%
[27]	2018	SVM vs RF	Multiple datasets for classification	Raspberry Pi 3 B, 1GB SRAM, Quad Core 1.2 GHz	ACC (SVM): 84.09% ACC (RF): 92.34%
[28]	2021	Framework: ML-MCU (Opt-SGD Algorithm)	Breast Cancer Wisconsin Dataset 567 Rows	Edge Device Not Mentioned Training Time: 3ms Flash Requirement: 228.84 kB SRAM Requirement: 27.38 kB	ACC: 83%
[29]	2019	Simple CNN	Custom Datasets: 3600 Images (3 Classes)	Raspberry Pi 3B+ 1 GB of RAM 1.4 GHz ARM A53	ACC (Leopards): 74% ACC (Humans): 77% ACC (Backgrounds): 72%
[30]	2020	InceptionV3	Multiple Datasets 33,984 Images	Raspberry Pi Model 4B, 2 seconds per Image	ACC: 94%

Chapter 3

Methodology

3.1 Overview

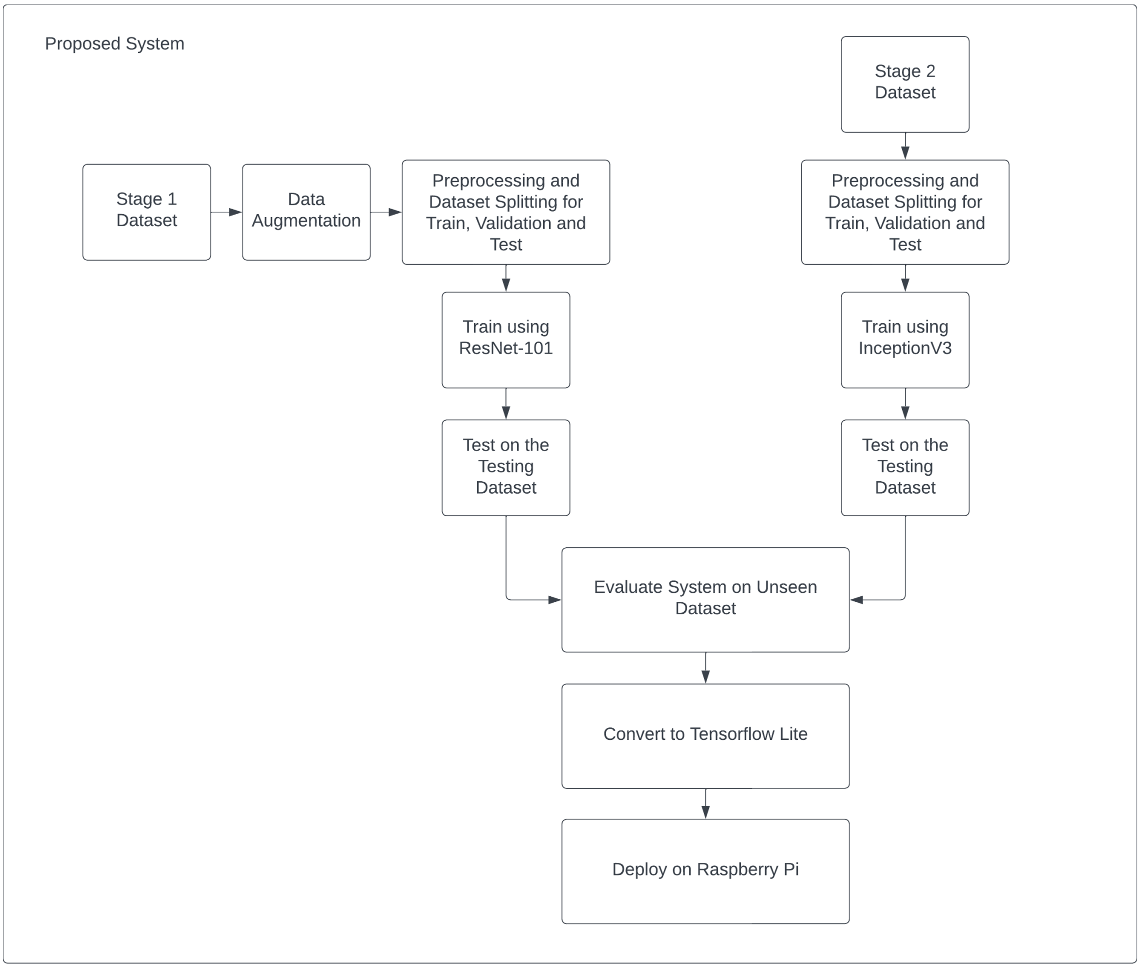

Figure 3.1: Block diagram for the proposed system.

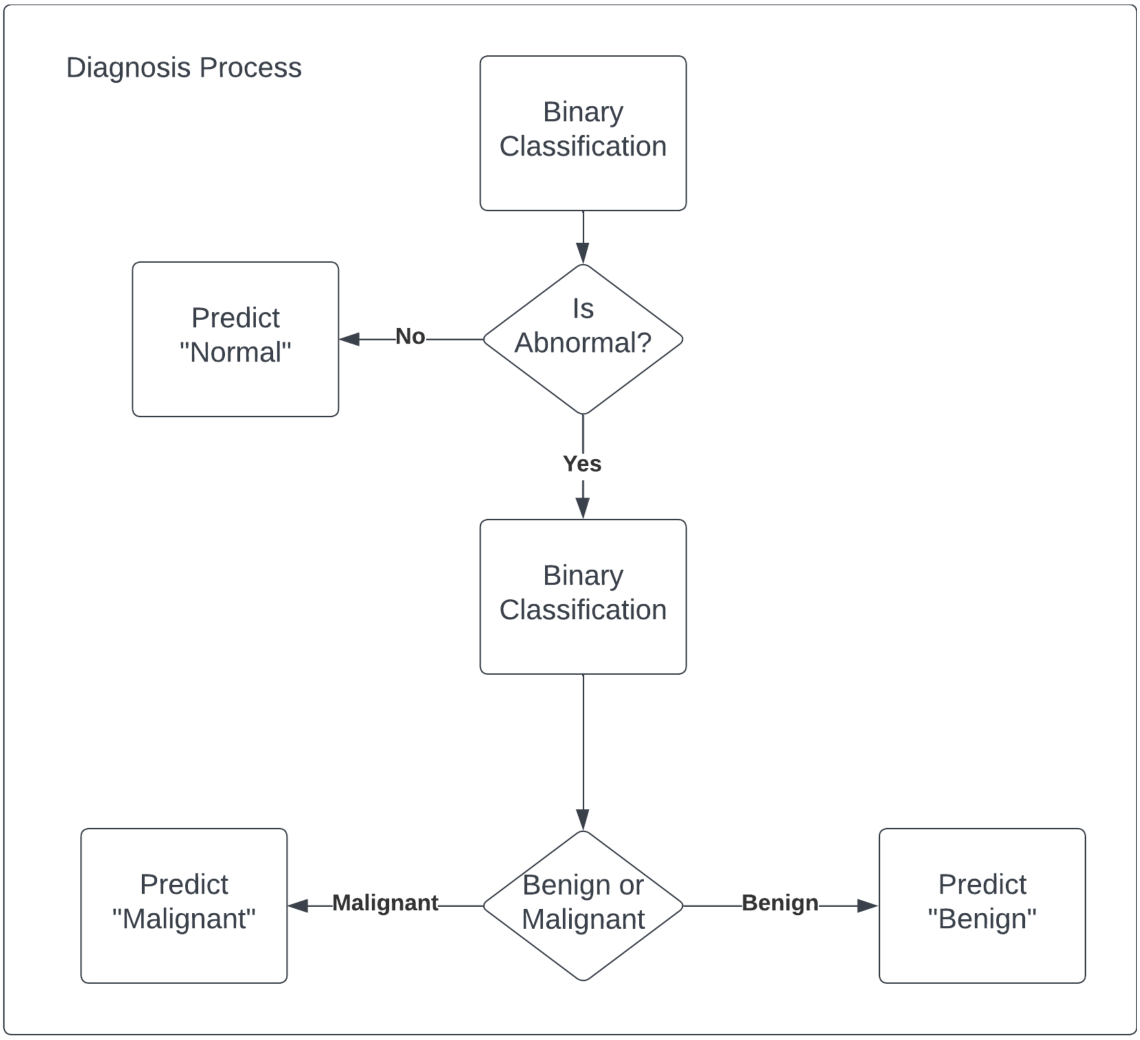

Figure 3.2: Block diagram for the diagnosis process.

3.2 Datasets

3.2.1 Dataset Details

This research combines six datasets from different countries, collected using various ultrasound devices. Initially, only the BUSI dataset was used for training and testing then Dataset (B) was introduced to assess how well the model could perform on unseen data. However, the results showed poor generalization, highlighting the need to include more datasets. The new datasets are: BUS_UC, BUS_WHU, BUS-UCLM, BUSBRA, the exact usage details can be found in Section 4.1.2.

3.2.2 Preprocessing

For the first stage, benign and malignant images were collected from all datasets mentioned except BUS-UCLM, as the images contained extra shapes that couldn't be cropped without potentially cropping out parts of the tumor too. The images were all combined into a single class, "abnormal," while the normal classes of BUS-UCLM and BUSI were combined to form the other class, "normal". Images were first cropped to remove unwanted shapes from the normal class in the BUS-UCLM dataset, and then converted to grayscale. The dataset was then manually cleaned to remove any remaining outliers. Lastly, to address class imbalance, the "normal" class was augmented using transformations such as flipping, random resized cropping, and random adjustments in brightness, contrast, saturation, and hue. For the second stage, benign and malignant images were only combined from BUSI, BUS_UC and BUSBRA, they were also manually cleaned to remove all outliers such as images with arrows pointing at the tumor.

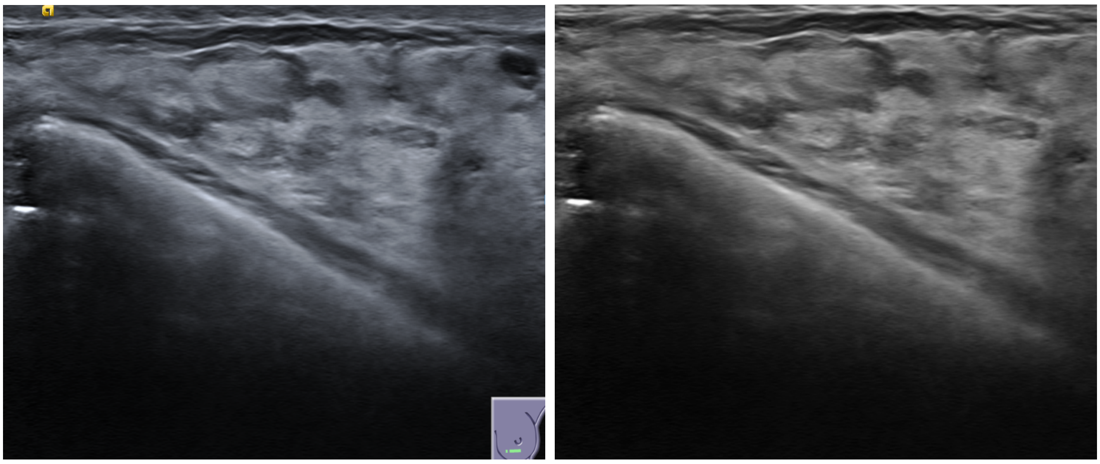

Original Image | Processed Image

Figure 3.3: Sample Image from BUS-UCLM before and after preprocessing.

3.3 Multi-stage Classification

3.3.1 Stage 1 — Classification: Normal vs Abnormal

The first step in the process involves using a pretrained ResNet-101 for determining whether an ultrasound image is within normal parameters or shows abnormalities suggestive of tumor presence. The dataset is divided into two classes: normal and abnormal. If an image is labelled as "normal" it's excluded from the rest of the process. The dataset was split randomly into 80% training, 10% testing and 10% validation. The model's fully connected layer was modified to add two dense layers with ReLU activation function, and two dropout layers and finally one last dense layer with a sigmoid activation function, the

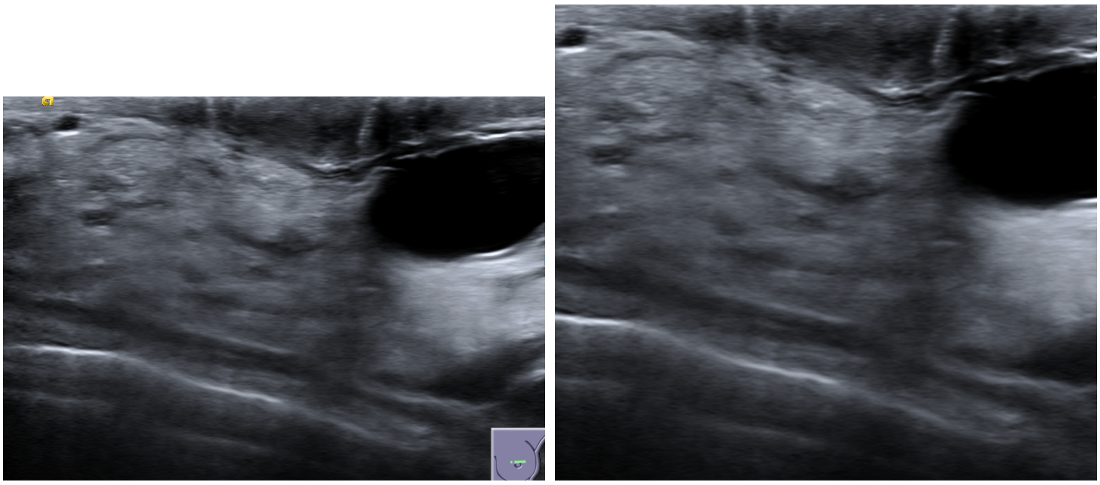

Original Image Cropped Image

Figure 3.4: Example of what could happen when cropping a non-normal image from BUS-UCLM.

dropout layers have a 50% drop chance to combat overfitting. In order to yield the most accurate results many tests were conducted using different hyperparameters and models, the exact results can be found in the results section in Chapter 4.

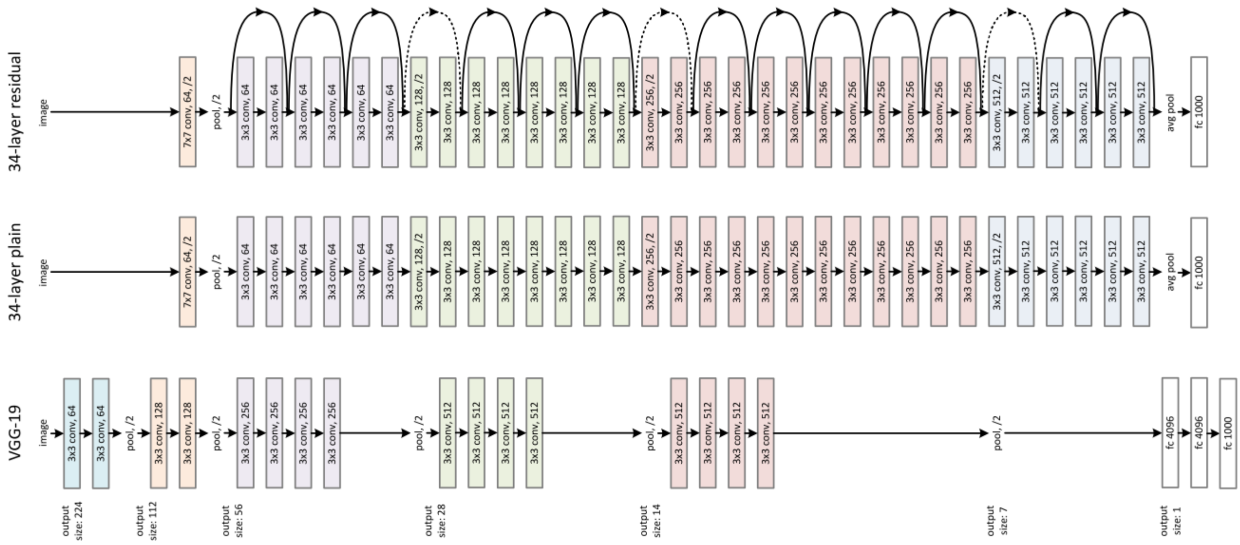

Figure 3.6: Illustration of the architecture of ResNet-34 in comparison to other CNNs [48].

3.3.2 Stage 2 — Classification: Benign vs Malignant

In the second stage of the diagnosis process, the dataset is divided into two classes: benign and malignant. The model used was a pretrained InceptionV3 Model, the weights used were from training it on the imagenet dataset. The dataset was split randomly into 80% training, 10% testing and 10% validation. This model's fully connected layer was also modified to add two dense layers with ReLU activation function, two dropout layers, two Batch Normalization layers immediately before the ReLU activation functions and finally one last dense layer with a sigmoid activation function, the dropout layers also have a 50% drop chance to combat overfitting.

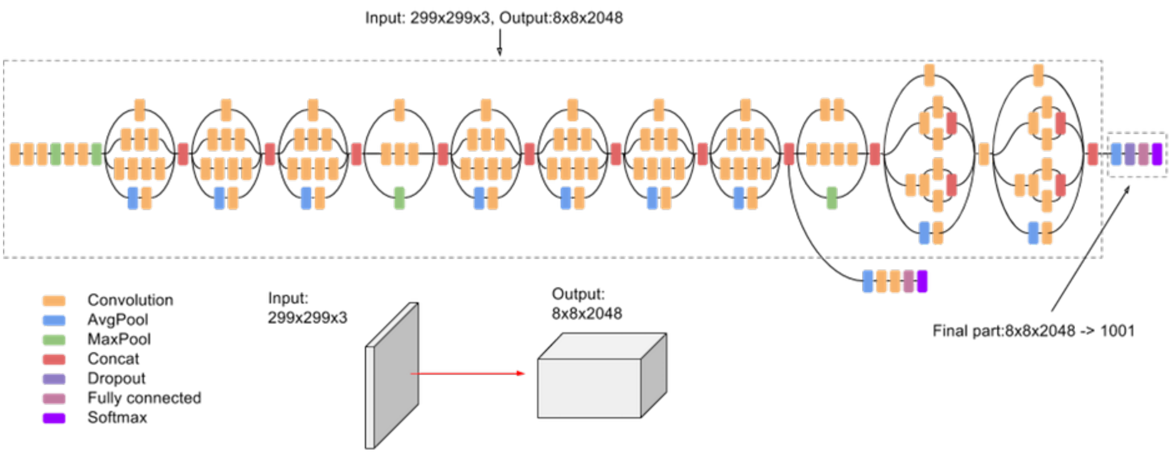

Figure 3.7: Illustration of the architecture of InceptionV3 [49].

3.4 Model Evaluation

After training the three models, they were tested on the unseen dataset which is Dataset B + 51 Images from BUSI from the "normal" class. Each ultrasound image undergoes a sequential process: first, it is fed into the initial classifier. If the model classifies the image as normal, it outputs the label and proceeds to the next image in the testing dataset. Otherwise, the image goes through the second stage which is another classifier to decide whether the image is "benign" or "malignant", the whole process can be seen in Figure 3.2.

3.5 Deployment on Raspberry Pi

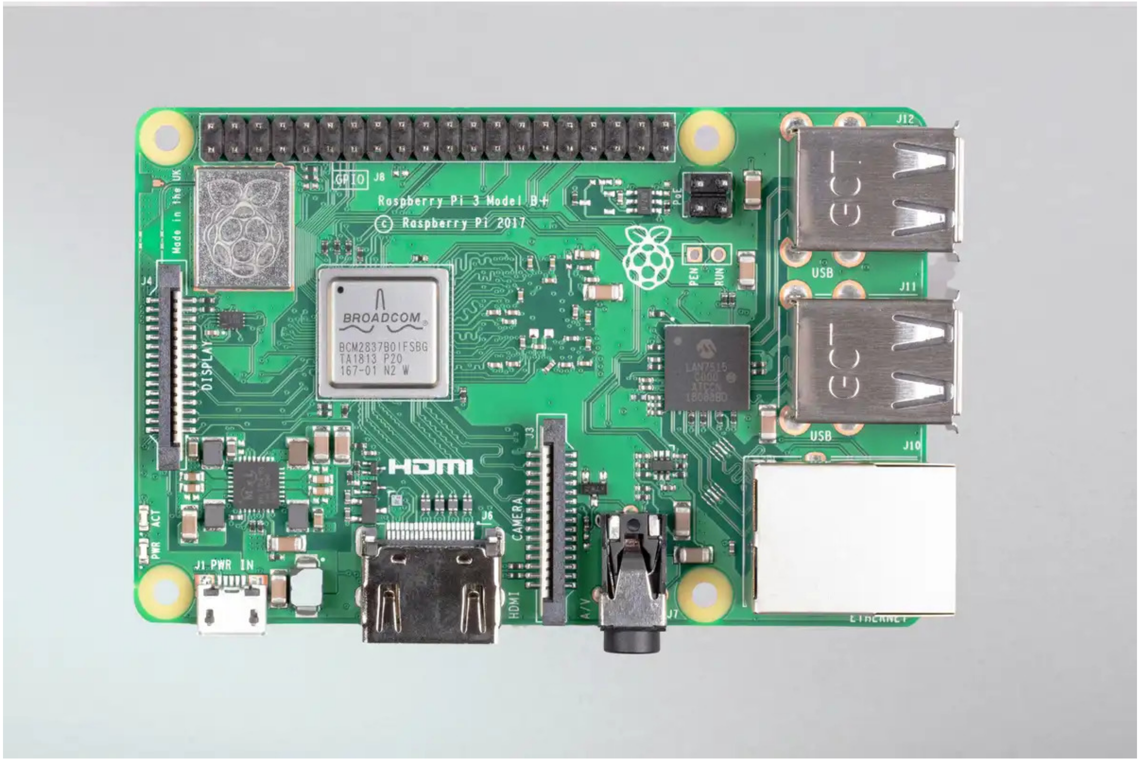

Figure 3.8: The Raspberry Pi 3 B+ Device [46].

3.5.1 Raspberry Pi Setup

For the deployment on the Raspberry Pi 3 B+, I began by configuring the device using the official Raspberry Pi Imager tool [44]. With this tool, I installed the latest release of Raspberry Pi OS (64-bit) onto the Raspberry Pi's 32GB microSD card. This step ensured that the operating system was up to date and compatible with the project requirements. After the installation, We created a python environment and started installing the necessary packages and updating the system packages to ensure optimal performance and security.

3.5.2 Optimization

The deployment process involves several key steps. Firstly, for optimization, we converted both Tensorflow models to Tensorflow Lite. Then, the lite version is transferred to the Raspberry Pi using a USB Flash Drive.

3.5.3 User Interface

The user interface was developed using Tkinter, a lightweight and user-friendly GUI toolkit for Python. The GUI was designed to allow users to input an image and immediately view the results after processing in a user-friendly manner. This streamlined approach provides users with a great experience, making the interaction with the application intuitive and easy.

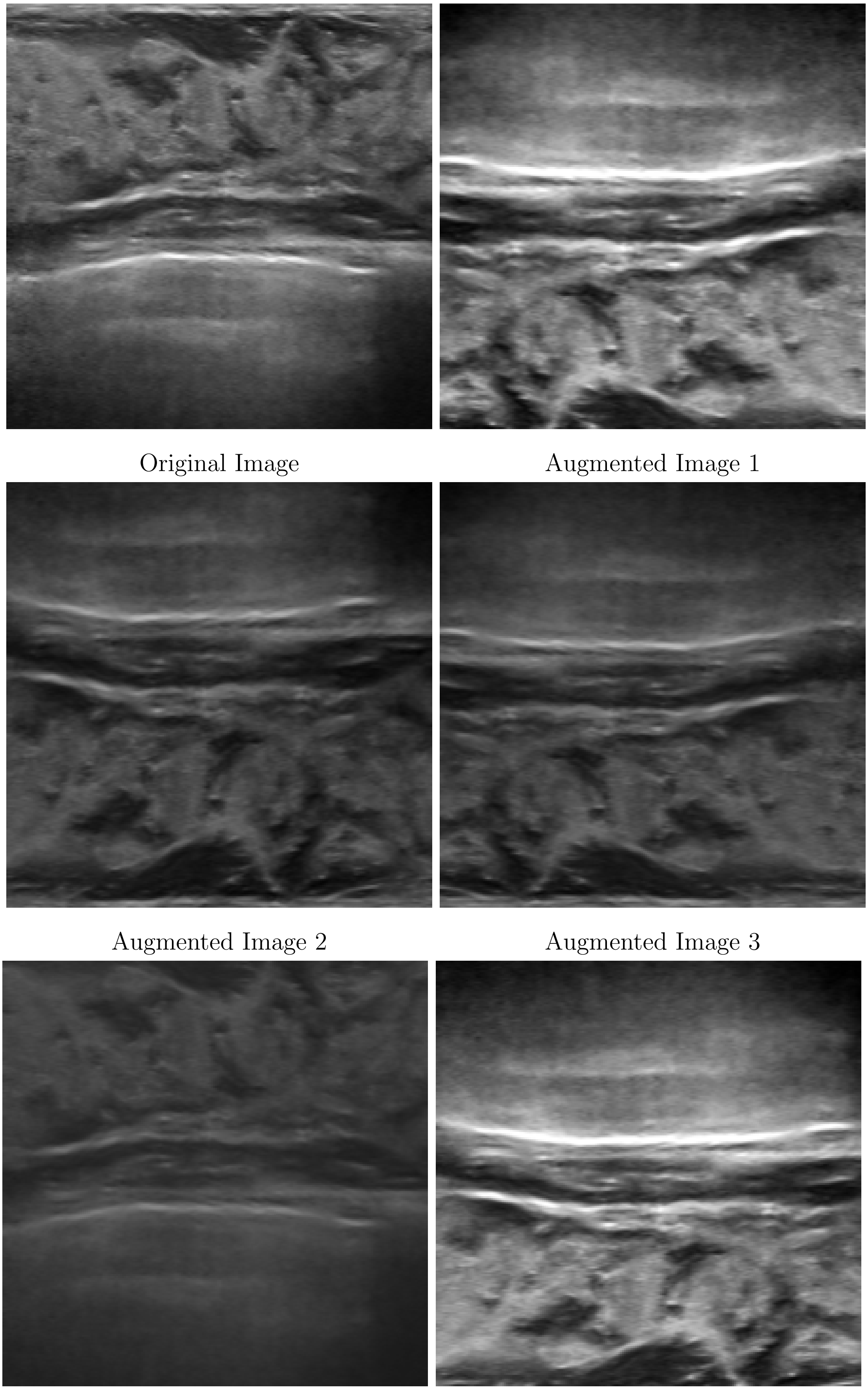

Original Image | Augmented Image 1

Augmented Image 2 | Augmented Image 3

Augmented Image 4 | Augmented Image 5

Figure 3.5: Examples of the Augmented Images.

Chapter 4

Results

4.1 Experimental Setup

4.1.1 Tools Used

Kaggle

Kaggle is an online platform that hosts data science competitions, datasets, and collaborative coding environments. It provides many accelerator options such as GPU T4 x2, GPU P100 and TPU VM v3-8.

Tensorflow

TensorFlow is an open-source software library for machine learning and AI.

Matplotlib

Matplotlib is a plotting library for Python. It provides functions for creating graphs and visualizing data.

Tkinter

Tkinter is a Python binding to the Tk GUI toolkit, which is the standard Python interface to the Tk GUI toolkit, it's used in this project to build a GUI for the users to navigate through.

Raspberry Pi 3 Model B+

The Raspberry Pi 3 Model B+ is a versatile and affordable single-board computer. The features include: a quad-core ARM Cortex-A53 CPU, 1GB of RAM, built-in Wifi and Bluetooth connectivity, GPIO pins for interfacing with external devices.

4.1.2 Dataset

- BUSI [31]: Collected in 2018 from 600 female patients. It consists of 780 PNG images and the ground truth images, with an average size of 500x500 pixels. The images are labelled benign, malignant or normal.

- Dataset B [32]: This dataset is managed by UDIAT-Centre Diagnostic, Corporacio Parc Tauli, Sabadell (Spain), it consists of 163 ultrasound images and the ground truth images, comprising 53 malignant and 110 benign cases.

- BUS_UC [33]: The BUS_UC dataset consists of 358 benign and 453 malignant tumor images, all at a resolution of 256 $\times$ 256 pixels. Sourced from Ultrasound Cases (ultrasoundcases.info), the dataset lacks ground truth images, but annotations by an experienced radiologist enable segmentation and classification tasks for both benign and malignant tumors.

- BUS_WHU [34]: Breast cancer ultrasound images were gathered from Renmin Hospital of Wuhan University's radiology department between December 2020 and December 2022. The dataset comprises 927 images, covering both benign and malignant cases from patients aged 17 to 79. Ethical approval was obtained from the hospital's ethics committee (WDRY2022-K217). Each image contains tumor regions with varying area and morphology features such as contrast, brightness, and fuzziness, making it suitable for segmentation tasks.

- BUS-UCLM [35]: The dataset comprises 683 breast ultrasound images from 38 patients, with 174 benign, 90 malignant, and 419 normal cases. Real Scans were obtained using a Siemens ACUSON S2000TM Ultrasound System between 2022 and 2023. Ground truth segmentation masks label lesions, aiding in breast cancer research and model development.

- BUSBRA [36]: The BUS dataset from Rio de Janeiro's National Institute of Cancer comprises 1875 ultrasound images from 1064 female patients, featuring 722 benign and 342 malignant cases. It includes BI-RADS assessments and manual lesion outlines for segmentation. The dataset offers 5- and 10-fold cross-validation partitions for CAD system evaluation.

Table 4.1: Original Datasets Comparison

Dataset	Sample 1	Sample 2	Sample 3
BUSI	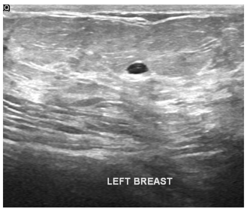	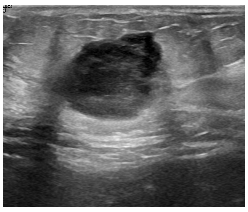	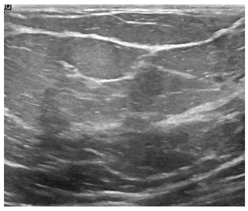
Dataset B	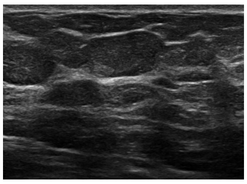	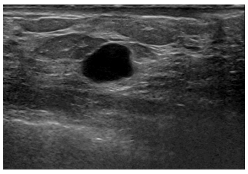	
BUS_UC	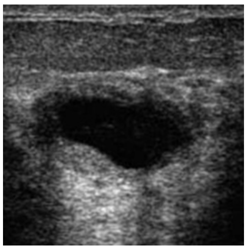	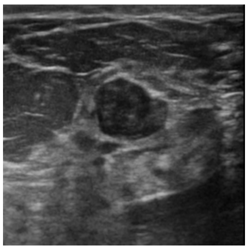	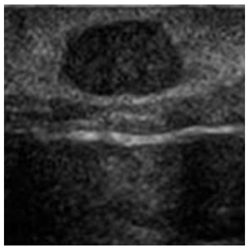
BUS_WHU	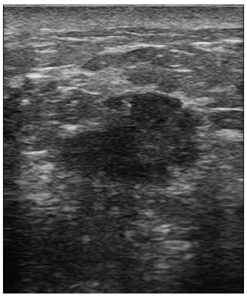		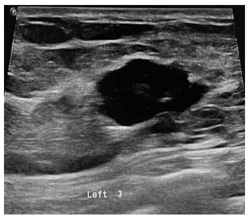
BUS-UCLM	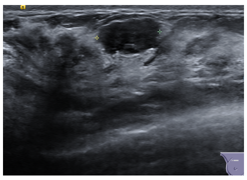	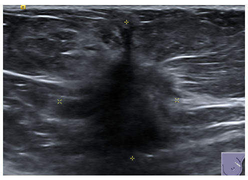	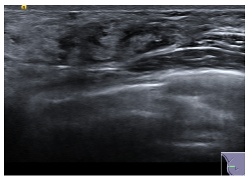
BUSBRA		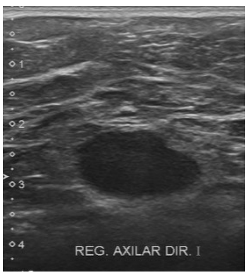	

Table 4.2: Summary of Dataset Usage for Stage 1.

Dataset	Total	Abnormal	Normal
BUSI	649	519	130
BUS_UC	811	811	0
BUS_WHU	927	927	0
BUS-UCLM	387	0	387
BUSBRA	1875	1875	0
Data Augmentation	3619	0	3619
Total	8268	4132	4136

Table 4.3: Summary of Dataset Usage for Stage 2.

Dataset	Total	Benign	Malignant
BUSI	557	350	207
BUS_UC	628	218	410
BUSBRA	1275	676	599
Total	2460	1244	1216

Table 4.4: Summary of Dataset Usage for the evaluation dataset.

Dataset	Total	Normal	Benign	Malignant
BUSI	45	45	0	0
Dataset B	120	0	77	43
Total	165	45	77	43

4.2 Experiments & Results

4.2.1 Experiments: Phase I

During this phase, we used a different multi-stage approach, starting with the same exact Stage which is classification to determine normal and abnormal masks. Then, if the image is abnormal, it gets segmented first, and the masked area of the image is used as an input for stage 3, which is the final classification stage. Only BUSI was used, and the loss mentioned in the three tables was calculated from the test dataset, which is a part of the BUSI dataset. Since PyTorch was used in this phase, the Lite model wouldn't be as optimized as it could have been with TensorFlow, which is why we converted the models to TensorFlow later in Phase 3 and changed the three-stages system.

In Stage 1, the division is 80% training, 10% testing, and 10% validation. Stage 2 comprises 85% training, 5% testing, and 10% validation. Stage 3 is divided exactly like Stage 1. When the models were tested on an unseen dataset (Dataset B), the model's accuracy dropped significantly. After concluding that the models memorized the dataset since most images looked similar, more datasets were needed to overcome this issue, so we started the preprocessing process for BUS_UC, BUS_WHU, BUS-UCLM, and BUSBRA.

Table 4.5: Summary of the experiments conducted during Stage 1. The optimizer used is ADAM with Cross-Entropy Loss.

Experiment	Model	LR	WD	Loss	ACC
1	ResNet-101	0.0001	0.00001	0.1148	0.9697
2	ResNet-101	0.0001	0.0001	0.1837	0.9394
3	ResNet-101	0.0001	0.0000	0.3507	0.8939
4	ResNet-152	0.0001	0.00001	0.2207	0.9091
5	ResNet-152	0.00008	0.0001	0.0494	0.9697
6	ResNet-101 + InceptionV4	0.0001	0.00001	0.2683	0.9091

Table 4.6: Summary of the experiments conducted during Stage 2. Dice Loss was used in all of them and no weight decay.

Experiment	Model	Optimizer	LR	Loss	IoU
7	DeepLabV3 - ResNet50	Adam	0.0005	0.2016	0.6328
8	DeepLabV3 - ResNet50	AdamW	0.0004	0.2413	0.6473
9	DeepLabV3 - ResNet101	AdamW	0.0001	0.3032	0.6373
10	DeepLabV3 - ResNet50	AdamW	0.0005	0.2471	0.6061

Table 4.7: Summary of the experiments conducted during Stage 3. The Optimizer used is ADAM.

Experiment	Model	LR	WD	Loss	ACC
11	ResNet101	0.0001	0.00001	0.0251	0.9841
12	InceptionV4	0.0001	0.00001	0.0179	1.0000
13	ResNet101 + InceptionV4	0.0001	0.00001	0.0181	0.9841

4.2.2 Experiments: Phase II

During this phase, we were still using PyTorch and the same multi-stage approach as in Phase 1. After concluding that the models memorized the dataset since most images looked similar in Phase 1, more datasets were needed to overcome this issue, so we started the preprocessing process for BUS_UC, BUS_WHU, BUS-UCLM, and BUSBRA.

Table 4.8: Summary of the experiments conducted during Stage 1. The optimizer used is ADAM with Cross-Entropy Loss.

Experiment	Model	LR	WD	Loss	ACC
14	ResNet101	0.0001	0.00001	0.0236	0.9953

Table 4.9: Summary of the experiments conducted during Stage 2. Dice Loss was used in all of them and no weight decay.

Experiment	Model	Optimizer	LR	Loss	Pixel ACC	IoU
15	DeepLabV3 - ResNet50	Adam	0.0002	0.1383	0.9666	0.7992

Table 4.10: Summary of the experiments conducted during Stage 3. The optimizer used is AdamW with Cross-Entropy Loss.

Experiment	Model	LR	WD	Loss	ACC
16	ResNet101	0.0001	0	0.3252	0.8731
17	InceptionV4	0.0001	0	0.2607	0.9067
18	ResNet101 + InceptionV4	0.0001	0	0.2566	0.9179

4.2.3 Experiments: Phase III

In this phase, the pipeline was adjusted to work with Tensorflow instead of PyTorch and the segmentation stage was removed because the results were significantly worse than the models available with PyTorch. This phase uses the proposed system discussed in Chapter 3 of the study. The dataset split is 70% training, 15% validation and 15% testing.

Table 4.11: Summary of the experiments conducted during Stage 1. The optimizer used is ADAM with Binary Cross-Entropy.

Experiment	Model	LR	Loss	ACC
19	ResNet101	0.00001	0.02252	0.9931
20	ResNet101	0.0001	0.0604	0.99
21	NASNetMobile	0.00001	0.0421	0.9878

Table 4.12: Summary of the experiments conducted during Stage 2. The loss function used was Cross-Entropy Loss. Both experiments 28 and 29 tried using Dropout = 0.7 instead of 0.5.

Experiment	Model	LR	WD	Optimizer	Loss	ACC
22	InceptionV3	0.0001	0	Adam	0.4263	0.85
23	InceptionV3	0.0001	0.01	AdamW	0.5273	0.83
24	InceptionV3	0.0001	0	AdamW	0.4231	0.85
25	InceptionV3	0.001	0	Nadam, 0.9	0.69161	0.5
26	InceptionV3	0.001	0	SGD	0.5632	0.75
27	InceptionV3	0.0001	0	AdamW	0.3804	0.86
28	InceptionResNetV2	0.0001	0	AdamW	0.4497	0.82
29	InceptionResNetV2	0.0001	0.0001	AdamW	0.51406	0.8226
30	NASNetMobile	0.00001	0	Adam	0.5897	0.67

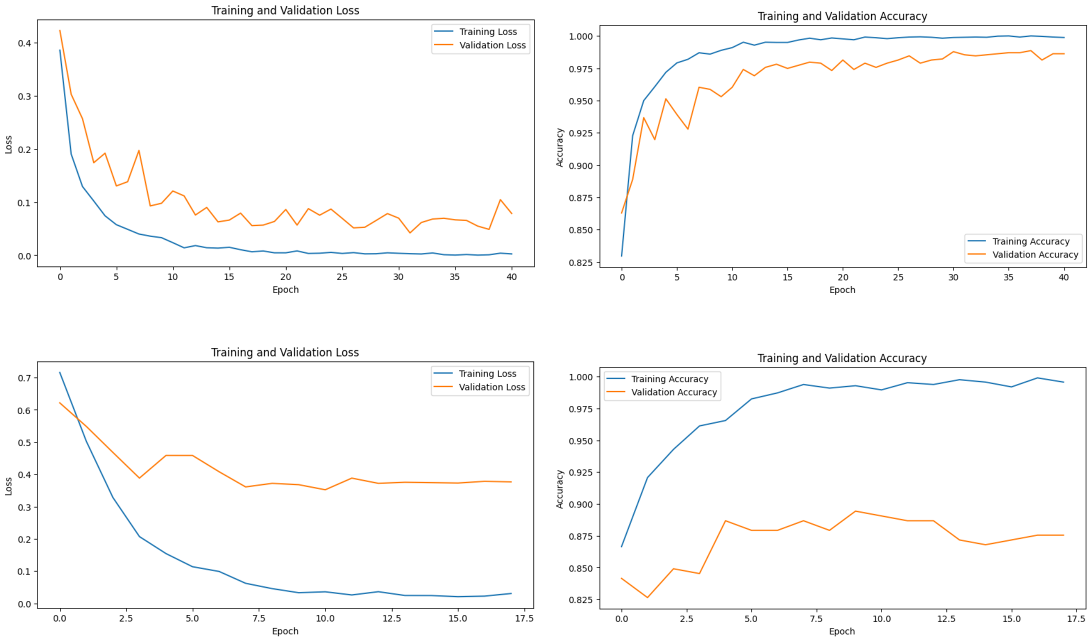

Figure 4.1: Results from both stages.

4.2.4 Final Results

The best results obtained in Stage 1 were achieved using ResNet-101 with a learning rate of 0.00001, which resulted in a loss of 0.02252 and an accuracy of 99.31%. In Stage 2, the highest performance was observed with InceptionV3 using the AdamW optimizer with a learning rate of 0.0001, yielding a loss of 0.3804 and an accuracy of 86%. By combining the models from both stages, we achieved an overall model accuracy of 88% on Dataset B which wasn't used in training at all. Finally, the model was able to process each image within seconds after being deployed on the Raspberry Pi device, allowing for instant diagnosis.

Chapter 5

Conclusion and Future Work

5.1 Conclusion

In conclusion, we have designed and trained a system for breast cancer diagnosis using ultrasound images. The integration of this model with a Raspberry Pi facilitated real-time diagnosis, while the development of a user-friendly interface ensured accessibility for healthcare professionals and end-users. This work has contributed to the development of an efficient device for the early detection of breast cancer, potentially improving patient outcomes through timely diagnosis and intervention. As discussed in Chapter 3, the GUI allows users to input an image, which then undergoes several stages in the pipeline. First, the image is preprocessed to prepare it for the classification models. Next, a classification algorithm identifies any abnormalities present. If abnormalities are detected, the system further classifies them as benign or malignant. Finally, the diagnostic outcome is displayed on the screen, providing rapid feedback to the user.

5.2 Limitations

However, this study encountered several limitations worth noting. Primarily, many of the datasets used in previous work were private datasets, making it very difficult to find high quality datasets for this and for other researches. Consequently, researchers often used data augmentation techniques on existing ultrasound images to address the scarcity of publicly available datasets. This reliance on augmented data may introduce variability and bias into the models and affecting the ability of the model to generalize and reliability of the findings. Another significant limitation was due to the edge device used, Raspberry Pi 3 B+ models only have 1GB of RAM, and usually advanced models that can achieve high accuracies are very resource-intensive so even trying to convert the model to TFLite was a challenge as even Kaggle's kernel sometimes failed in converting them due to memory issues.

5.3 Future Work

Addressing the limitations of this study opens up several paths for future research. Firstly, efforts should be directed towards acquiring or creating more diverse and high-quality datasets for training and evaluation purposes. This would involve collaborating with medical institutions to access larger and more representative datasets that should be made public for researchers.

Additionally, exploring alternative edge devices with higher computational capabilities could improve and simplify the process of deploying advanced models for real-world applications. Moreover, investigating techniques to optimize model architecture and employ compression methods could effectively reduce memory and computational constraints, especially in edge device deployment scenarios.

Bibliography

[1] I. PACAL, "Deep learning approaches for classification of breast cancer in ultrasound (us) images," *Journal of the Institute of Science and Technology*, vol. 12, no. 4, p. 1917–1927, 2022.

[2] J. Li, Y. Bu, S. Lu, H. Pang, C. Luo, Y. Liu, and L. Qian, "Development of a deep learning–based model for diagnosing breast nodules with ultrasound," *Journal of Ultrasound in Medicine*, vol. 40, no. 3, pp. 513–520, 2021.

[3] H. Tanaka, S.-W. Chiu, T. Watanabe, S. Kaoku, and T. Yamaguchi, "Computer-aided diagnosis system for breast ultrasound images using deep learning," *Physics in Medicine & Biology*, vol. 64, p. 235013, dec 2019.

[4] N. Sirjani, M. Ghelich Oghli, M. Kazem Tarzamni, M. Gity, A. Shabanzadeh, P. Ghaderi, I. Shiri, A. Akhavan, M. Faraji, and M. Taghipour, "A novel deep learning model for breast lesion classification using ultrasound images: A multicenter data evaluation," *Physica Medica: European Journal of Medical Physics*, vol. 107, 2023.

[5] A. S. Becker, M. Mueller, E. Stoffel, M. Marcon, S. Ghafoor, and A. Boss, "Classification of breast cancer in ultrasound imaging using a generic deep learning analysis software: a pilot study," *British Journal of Radiology*, vol. 91, p. 20170576, 01 2018.

[6] W. Al-Dhabyani, M. Gomaa, H. Khaled, and A. Fahmy, "Deep learning approaches for data augmentation and classification of breast masses using ultrasound images," *International Journal of Advanced Computer Science and Applications*, vol. 10, no. 5, 2019.

[7] T. Fujioka, K. Kubota, M. Mori, Y. Kikuchi, L. Katsuta, M. Kasahara, G. Oda, T. Ishiba, T. Nakagawa, and U. Tateishi, "Distinction between benign and malignant breast masses at breast ultrasound using deep learning method with convolutional neural network," *Japanese Journal of Radiology*, vol. 37, no. 6, pp. 466–472, 2019.

[8] K. Jabeen, M. A. Khan, M. Alhaisoni, U. Tariq, Y.-D. Zhang, A. Hamza, A. Mickus, and R. Damaševičius, "Breast cancer classification from ultrasound images using probability-based optimal deep learning feature fusion," *Sensors*, vol. 22, no. 3, 2022.

[9] K. Inoue, C. Yamanaka, A. Kawasaki, K. Koshimizu, T. Sasaki, and T. Doi, "Computer aided detection of breast cancer on ultrasound imaging using deep learning," *Ultrasound in Medicine and Biology*, vol. 43, no. S19, 2017.

[10] S. W. Cho, N. R. Baek, and K. R. Park, "Deep learning-based multi-stage segmentation method using ultrasound images for breast cancer diagnosis," *Journal of King Saud University - Computer and Information Sciences*, vol. 34, no. 10, Part B, pp. 10273–10292, 2022.

[11] M. G. Lanjewar, K. G. Panchbhai, and L. B. Patle, "Fusion of transfer learning models with lstm for detection of breast cancer using ultrasound images," *Computers in Biology and Medicine*, vol. 169, p. 107914, 2024.

[12] R. Tian, G. Lu, S. Tang, L. Sang, H. Ma, W. Qian, and W. Yang, "Benign and malignant classification of breast tumor ultrasound images using conventional radiomics and transfer learning features: A multicenter retrospective study," *Medical Engineering & Physics*, vol. 125, p. 104117, 2024.

[13] Y. Wang, E. J. Choi, Y. Choi, H. Zhang, G. Y. Jin, and S.-B. Ko, "Breast cancer classification in automated breast ultrasound using multiview convolutional neural network with transfer learning," *Ultrasound in Medicine and Biology*, vol. 46, no. 5, pp. 1119–1132, 2020.

[14] I. B. AHMED, W. OUARDA, and C. B. AMAR, "Enhanced computer-aided diagnosis model on ultrasound images through transfer learning and data augmentation techniques for an accurate breast tumors classification," *Procedia Computer Science*, vol. 225, pp. 3938–3947, 2023. 27th International Conference on Knowledge Based and Intelligent Information and Engineering Sytems (KES 2023).

[15] Y. Luo, Q. Huang, and L. Liu, "Classification of tumor in one single ultrasound image via a novel multi-view learning strategy," *Pattern Recognition*, vol. 143, p. 109776, 2023.

[16] M. H. Yap, G. Pons, J. Martí, S. Ganau, M. Sentís, R. Zwiggelaar, A. K. Davison, and R. Martí, "Automated breast ultrasound lesions detection using convolutional neural networks," *IEEE Journal of Biomedical and Health Informatics*, vol. 22, pp. 1218–1226, July 2018.

[17] A. Vakanski, M. Xian, and P. E. Freer, "Attention-enriched deep learning model for breast tumor segmentation in ultrasound images," *Ultrasound in Medicine and Biology*, vol. 46, no. 10, pp. 2819–2833, 2020.

[18] M. Ragab, A. Albukhari, J. Alyami, and R. F. Mansour, "Ensemble deep-learning-enabled clinical decision support system for breast cancer diagnosis and classification on ultrasound images," *Biology*, vol. 11, no. 3, 2022.

[19] X. Qian, J. Pei, H. Zheng, X. Xie, L. Yan, H. Zhang, C. Han, X. Gao, H. Zhang, W. Zheng, Q. Sun, L. Lu, and K. K. Shung, "Prospective assessment of breast cancer risk from multimodal multiview ultrasound images via clinically applicable deep learning," *Nature Biomedical Engineering*, vol. 5, no. 6, pp. 522–532, 2021.

[20] Y. Li, H. Gu, H. Wang, P. Qin, and J. Wang, "Busnet: A deep learning model of breast tumor lesion detection for ultrasound images," *Frontiers in Oncology*, vol. 12, 2022.

[21] S.-H. Chen, Y.-L. Wu, C.-Y. Pan, L.-Y. Lian, and Q.-C. Su, "Breast ultrasound image classification and physiological assessment based on googlenet," *Journal of Radiation Research and Applied Sciences*, vol. 16, no. 3, p. 100628, 2023.

[22] Y.-C. Zhu, A. AlZoubi, S. Jassim, Q. Jiang, Y. Zhang, Y.-B. Wang, X.-D. Ye, and H. DU, "A generic deep learning framework to classify thyroid and breast lesions in ultrasound images," *Ultrasonics*, vol. 110, p. 106300, 2021.

[23] S. Hossain, S. Azam, S. Montaha, A. Karim, S. S. Chowa, C. Mondol, M. Zahid Hasan, and M. Jonkman, "Automated breast tumor ultrasound image segmentation with hybrid unet and classification using fine-tuned cnn model," *Heliyon*, vol. 9, no. 11, p. e21369, 2023.

[24] S. B. and A. Pulikala, "Aapfc-busnet: Hierarchical encoder–decoder based cnn with attention aggregation pyramid feature clustering for breast ultrasound image lesion segmentation," *Biomedical Signal Processing and Control*, vol. 91, p. 105969, 2024.

[25] X. Qi, F. Yi, L. Zhang, Y. Chen, Y. Pi, Y. Chen, J. Guo, J. Wang, Q. Guo, J. Li, Y. Chen, Q. Lv, and Z. Yi, "Computer-aided diagnosis of breast cancer in ultrasonography images by deep learning," *Neurocomputing*, vol. 472, pp. 152–165, 2022.

[26] S. Zahir, A. Amir, N. A. H. Zahri, and W. C. Ang, "Applying the deep learning model on an iot board for breast cancer detection based on histopathological images," *Journal of Physics: Conference Series*, vol. 1755, p. 012026, feb 2021.

[27] M. T. Yazici, S. Basurra, and M. M. Gaber, "Edge machine learning: Enabling smart internet of things applications," *Big Data and Cognitive Computing*, vol. 2, no. 3, 2018.

[28] B. Sudharsan, J. G. Breslin, and M. I. Ali, "Ml-mcu: A framework to train ml classifiers on mcu-based iot edge devices," *IEEE Internet of Things Journal*, vol. 9, pp. 15007–15017, Aug 2022.

[29] B. H. Curtin and S. J. Matthews, "Deep learning for inexpensive image classification of wildlife on the raspberry pi," in *2019 IEEE 10th Annual Ubiquitous Computing, Electronics & Mobile Communication Conference (UEMCON)*, pp. 0082–0087, Oct 2019.

[30] I. A. Zualkernan, S. Dhou, J. Judas, A. R. Sajun, B. R. Gomez, L. A. Hussain, and D. Sakhnini, "Towards an iot-based deep learning architecture for camera trap image classification," in *2020 IEEE Global Conference on Artificial Intelligence and Internet of Things (GCAIoT)*, pp. 1–6, Dec 2020.

[31] W. Al-Dhabyani, M. Gomaa, H. Khaled, and A. Fahmy, "Dataset of breast ultrasound images," *Data in Brief*, vol. 28, p. 104863, 2020.

[32] M. H. Yap, G. Pons, J. Marti, S. Ganau, M. Sentis, R. Zwiggelaar, A. K. Davison, and R. Marti, "Automated breast ultrasound lesions detection using convolutional neural networks," *IEEE Journal of Biomedical and Health Informatics*, 2017.

[33] A. Iqbal, "Bus_uc," 2023.

[34] J. Huang, J. Zhang, Y. Zhang, X. Li, X. Ma, J. Deng, H. Shen, D. Wang, L. Mei, and C. Lei, "Busi_whu: Breast cancer ultrasound image dataset," 2023.

[35] N. Vallez, G. Bueno, O. Deniz, M. A. Rienda, and C. Pastor, "Bus-uclm: Breast ultrasound lesion segmentation dataset," 2024.

[36] W. Gómez-Flores, M. Gregorio-Calas, and W. Coelho de Albuquerque Pereira, "Busbra: A breast ultrasound dataset for assessing computer-aided diagnosis systems," *Medical Physics*, vol. 51, no. 4, pp. 3110–3123, 2024.

[37] "Worldwide cancer data." https://www.wcrf.org/cancer-trends/worldwide-cancer-data/#:~:text=Find%20information%20about%20world%20cancer,and%208.8%20million%20in%20women. Accessed on March 4, 2024.

[38] D. Crosby, S. Bhatia, K. M. Brindle, L. M. Coussens, C. Dive, M. Emberton, S. Esener, R. C. Fitzgerald, S. S. Gambhir, P. Kuhn, T. R. Rebbeck, and S. Balasubramanian, "Early detection of cancer," *Science*, vol. 375, no. 6586, p. eaay9040, 2022.

[39] N. Tekin, A. Aris, A. Acar, S. Uluagac, and V. C. Gungor, "A review of on-device machine learning for iot: An energy perspective," *Ad Hoc Networks*, vol. 153, p. 103348, 2024.

[40] W. Xing and D. Du, "Dropout prediction in moocs: Using deep learning for personalized intervention," *Journal of Educational Computing Research*, vol. 57, p. 073563311875701, 03 2018.

[41] J. Lemley, S. Bazrafkan, and P. Corcoran, "Transfer learning of temporal information for driver action classification," p. 0, 04 2017.

[42] International Agency for Research on Cancer, "Breast cancer screening: Breast imaging - breast atlas," 2024. Accessed: 2024-05-18.

[43] Jewel Women's Center, "Early pregnancy ultrasound," 2024. Accessed: 2024-05-18.

[44] Raspberry Pi Foundation, "Raspberry Pi Software." https://www.raspberrypi.com/software/. Accessed: May 2024.

[45] J. Brownlee, "Overfitting in machine learning models." https://machinelearningmastery.com/overfitting-machine-learning-models/. Accessed: May 2024.

[46] "Raspberry Pi 3 Model B+." https://www.raspberrypi.com/products/raspberry-pi-3-model-b-plus/. Accessed: May 2024.

[47] "Desmos." https://www.desmos.com/. Accessed: May 2024.

[48] K. He, X. Zhang, S. Ren, and J. Sun, "Deep residual learning for image recognition," 2015.

[49] P. with Code, "Inception-v3." https://paperswithcode.com/method/inception-v3. Accessed: May 18, 2024.